infrastructures

MDPI

Article

A New Prediction Model of Cutterhead Torque in Soil Strata Based on Ultra-Large Section EPB Pipe Jacking Machine

Jianwei Lu [1,2], Bo Sun [1], Qiuming Gong [2,*], Tiantian Song [1], Wei Li [1,*], Wenpeng Zhou [3] and Yang Li [4]

[1] Shenzhen Metro Group Co., Ltd., Shenzhen 518038, China; jianweilu.geo@gmail.com (J.L.); sunbo@shenzhenmc.com (B.S.); stt5@163.com (T.S.)
[2] Key Laboratory of Urban Security and Disaster Engineering of Ministry of Education, Beijing University of Technology, Beijing 100124, China
[3] China Water Resources and Hydropower Eleventh Engineering Bureau Co., Ltd., Zhenzhou 450001, China; zhouwp0629@163.com
[4] China Railway Engineering Equipment Group Co., Ltd., Zhenzhou 450047, China; thinkweed@foxmail.com
* Correspondence: gongqiuming@bjut.edu.cn (Q.G.); weiliyy@126.com (W.L.)

Abstract: Cutterhead torque is a key operational parameter for earth pressure balance (EPB) TBM tunneling in soil strata. The effective management of cutterhead torque can significantly maintain face stability and ensure the tunneling machine operates steadily. The Shenzhen Metro Line 12 project at Shasan Station utilized the world's largest rectangular pipe jacking machine for constructing the subway station. This project has enabled the collection of relevant data to analyze the factors influencing cutterhead torque and to establish a predictive model. The data encompass an abundant array of cutterhead design parameters, operational parameters, properties of the excavated soil, and environmental factors, revealing the distribution characteristics of cutterhead torque during tunneling. The correlation between various factors and cutterhead torque has been examined. By employing multiple regression analysis and a Levenberg–Marquardt (L-M) algorithm-based neural network, an optimal prediction model for EPB cutterhead torque has been developed. This prediction model incorporates various factors, including cutterhead diameter, RPM, soil chamber pressure, soil shear strength, and the soil consistency index. And the degree of influence of each factor on the cutter torque was also revealed. The prediction results demonstrated good accuracy compared to previous models, providing valuable insights and guidance for EPB TBMs or pipe jacking machines operating in soil strata. The current limitations of this model and suggestions for future work have also been addressed.

Keywords: cutterhead torque; pipe jacking machine; EPB TBM; prediction model; correlation analysis; neural network

check for updates

Citation: Lu, J.; Sun, B.; Gong, Q.; Song, T.; Li, W.; Zhou, W.; Li, Y. A New Prediction Model of Cutterhead Torque in Soil Strata Based on Ultra-Large Section EPB Pipe Jacking Machine. *Infrastructures* **2024**, *9*, 212. https://doi.org/10.3390/infrastructures9120212

Academic Editor: Youssef Diab

Received: 25 October 2024
Revised: 17 November 2024
Accepted: 20 November 2024
Published: 21 November 2024

Copyright: © 2024 by the authors. Licensee MDPI, Basel, Switzerland. This article is an open access article distributed under the terms and conditions of the Creative Commons Attribution (CC BY) license (https://creativecommons.org/licenses/by/4.0/).

1. Introduction

EPB Tunnel Boring Machines (TBMs) are commonly used in soft ground due to their advantages of speed, safety, and environmental friendliness. They have become the most employed type of TBM [1]. EPB TBMs effectively maintain face stability and control surface settlement through careful management of soil chamber pressure, achieved via cutterhead control. Key operational parameters for EPB TBM include both control parameters (such as thrust, cutterhead RPM, soil chamber pressure, and screw conveyor RPM) and response parameters (including cutterhead torque, penetration, and advance rate). These are influenced by geological conditions and the selected control parameters [2,3]. Cutterhead torque is crucial for overcoming face resistance, cutting soil, and regulating muck flow into the soil chamber. Effective torque management is essential for smooth excavation, reducing tool wear, and preventing equipment overload [4]. However, the torque requirements of an EPB TBM cutterhead depend on several factors, such as soil type, tool design, cutterhead diameter, RPM, and soil chamber pressure. A comprehensive understanding of these

factors is essential for optimizing cutterhead performance and maximizing excavation efficiency, making a reliable torque prediction critical to EPB TBM tunneling success.

Various models, including those by Bruland [5], Rostami and Ozdemir [6], Cigla and Ozdemir [7], An et al. [8], and Zare Naghadehi et al. [9], have been developed to predict parameters such as cutterhead torque for hard rock TBM tunneling. These models correlate machine performance with geological rock mass characteristics. Additionally, some researchers have predicted cutterhead torque in mixed-face geological conditions by analyzing diverse rock properties [10–13]. Numerous studies have explored the torque characteristics of EPB TBM cutterheads under various soil conditions and surrounding environmental conditions, with models broadly classified as either theoretical or empirical.

In theoretical models, Shi et al. (2011) [14] and Wang et al. (2012) [1] proposed a physical model-based analytical formula to predict EPB TBM torque by dividing the cutterhead into sections and analyzing soil interaction-generated torque. Subsequent researchers [1,15,16] further refined the model proposed by [14]. Similarly, Xu et al. (2010) [17] and Lin (2006) [18] developed similar models. Zhang et al. [19] took a different approach to the cutterhead torque equation by incorporating the nonlinear pressure at the cutterhead front and the effect of the penetration rate. Among empirical models, Krause (1987) [20] presented a widely used model that calculates cutterhead torque based on the cutterhead diameter and an empirical coefficient, α, generally ranging from 10 to 25 for EPB TBMs and 8 to 20 for slurry TBMs. Ates et al. (2014) [4] also proposed a diameter-based model, while Avunduk and Copur (2018) [21] introduced a torque prediction model incorporating soil shear strength and a consistency index. Ramoni and Anagnostou [22,23] made some studies to analyze the empirical method for predicting the thrust and torque requirement of TBMs in squeezing ground. The calculation formulas for each model are shown in Table 1.

Former studies have primarily focused on TBMs, analyzing cutterhead operational parameters with a relatively uniform machine design, excavation conditions, and surrounding environments. Zhang et al. (2014) [24] compared field data with Krause's empirical model, noting that the calculated torque ranged between 180% and 460% of the actual average torque, due to the large safety margins embedded in empirical models. Therefore, a more comprehensive cutterhead torque prediction model, incorporating geological, environmental, and equipment design factors, is needed for accurate forecasting.

Rectangular pipe jacking tunnels, with their high utilization of cross-sectional area, shallow depth, and minimal impact on surrounding environments, represent a promising development in urban short-distance tunneling technology [25–29]. Advances in rectangular pipe jacking machines have enabled larger cross-sections for diverse construction needs. These rectangular pipe jacking machines are typically equipped with multiple cutterheads of varying diameters for full-face excavation. Compared to TBMs, the larger cross-section of rectangular pipe jacking machines introduces additional factors affecting cutterhead torque, including geological conditions, cutterhead design and arrangement, and soil chamber pressure, allowing for an abundant database for torque analysis and prediction.

This study aims to create a more comprehensive EPB TBM cutterhead torque prediction model, accounting for geological, environmental, and equipment design factors, to improve theoretical accuracy in EPB TBM tunneling in soil strata. This research is based on the Shasan Station, part of Shenzhen Metro Line 12 in China, where construction involved the rectangular pipe jacking machine with the world's largest excavation area. By collecting design parameters and operational parameters along with soil properties, this study conducted univariate regression analysis to identify the correlation between each influencing factor and torque, followed by performed multiple regression analyses and a Levenberg-Marquardt (L-M) algorithm-based neural network to develop a torque prediction model.

Table 1. The summary of cutterhead torque prediction model.

Authors	Friction Torque on Frontal Surface	Friction Torque on Circular Surface	Friction Torque on Back Surface	Cutting Torque	Shearing Torque on	Torque of Rotational Bearing
Shi et al. (2011) [14]	$T_1 = \frac{\pi D^3}{12} K_0 f \gamma H (1-\eta)$	$T_2 = \frac{\pi D^2}{4} f \gamma H W (1+K_0)$	$T_3 = \frac{\pi D^3}{12} K_0 f \gamma H (1-\eta) f_{\Delta p}$	$T_4 = \sum_{i-1}^{n} F_{ci} r_i$	$T_5 = \frac{\pi D^3}{12} \cdot k_q \cdot \eta \cdot \tau$	$T_6 = \sum_{i=1}^{n_b} \gamma (H - L_i sin\theta_b) \cdot D_b \cdot L_b \cdot f_c \cdot n_b \cdot R_b$
Godinez et al. (2015) [15]	Based on Shi et al. (2011), the soil arch effect is considered.					
Koohsari et al. (2023) [16]	$T = \omega(T_1 + T_2 + T_3 + T_5 + T_{Other})$. Based on Shi et al. (2011), the RPM is considered.					
Xu et al. (2010) [17]	$T_2 = (1-\eta)\mu p_0 e^{Al} \frac{\pi D^3}{12}$	$T_3 = \frac{\pi D^2}{8} \frac{1}{2} (c + N\tan\varphi) l_k$	-	$T_1 = \sum_{i=1}^{n} Q_i r_i$	$T_4 = \eta \frac{C_\tau \pi D^3}{6}$	-
Lin (2006) [18]	$T_{1a} = \frac{\pi D^3}{12} K_0 f \gamma H (1-\eta)$	$T_{1b} = \frac{\pi D^2}{4} f \gamma H W (1+K_0)$	$T_2 = \frac{\pi D^3}{12} K_0 f' \gamma H (1-\eta) k$	-	-	$T_3 = k \sum_{n} \gamma H D_b L_b R_b f'$
Zhang et al. (2014) [24]	$T_1 = \frac{\pi G f_1 (1-\eta)}{1-\mu} + (1-\eta) \frac{2}{3} \pi R^3 f_1 K_0 \gamma H$	$T_3 = 2\pi R^2 t f_4 P_m$	-	$T_2 = \frac{1}{2} \delta c R^2 + \frac{2RG\delta^2 \tan\varphi}{\pi(1-\eta)}$	-	$T_4 = n_b \pi D_b L_b R_b f' P_m$
Krause (1987) [20]	$T = \alpha \cdot D^3$ ($EPB\ TBM:\ 10 \leq \alpha \leq 25$, $slurry\ TBM:\ 8 \leq \alpha \leq 20$)					
Avunduk and Copur (2018) [21]	$T = 4.28 S_u + 270 I_c + 230$					
Ates et al. (2014) [4]	$T = 13.438 D^{3.154}$					

Note: D is cutterhead diameter, K_0 is the coefficient of lateral earth pressure, f is the coefficient of dynamic friction, γ is the volume weight, H is the depth, η is the opening ratio of cutterhead, W is the width of cutterhead, $f_{\Delta p}$ is the coefficient related to the difference between inner and outer pressures, F_{ci} is the resistance force applied on the cutter i, n is the number of the cutter fixed on cutterhead τ is the shear strength of the soil, k_q is a reduced coefficient related to shear area, n_b is the number of the agitating bars, R_b is the distance between the agitating bar and the centerline of shield, θ_b is the angle of the plane through the axes of the bar and the shield with respect to the horizontal plane, D_b is the diameter of the agitating bar, L_b is the length of the agitating bar, f_c is the friction factor between the improved earth and the steel bar, ω is the rotational speed, p_0 is the chamber earth pressure, A is constant, ν is Poisson's ratio of soil, φ is internal friction angle of soil, l is the length of chamber, c is the soil cohesion, N is the normal earth pressure at rest acting on the cutterhead, Q_i is the tangential force of the tool, r_i is the distance of each tool from the center of the cutterhead, C_τ is the shear strength of the muck, k is the ratio of the earth pressure in the chamber to the earth pressure on the tunnel face, and f' is the friction coefficient between the cutterhead, the stirring rod, and the muck, P_m is the average soil pressure on the shield, S_u is the vane shear strength, I_c is the consistency index.

The paper is organized as follows: The second section provided background on the supporting engineering project, including the metro station, geological conditions, and the combined tunnel boring machine used. The third section analyzed the torque parameters of various cutterheads and identified how these characteristics change at different excavation stages. The fourth section established a database, performed univariate correlation analysis to identify relationships, and applied both multiple linear regression and a neural network based on the Levenberg–Marquardt algorithm to develop cutterhead torque prediction models. The fifth section evaluated the applicability and interpretability of the prediction models to identify the most suitable one. In Section 5, conclusions were drawn.

2. Project Overview

2.1. Project Description

The Shasan Station of Shenzhen Metro Line 12 Phase II is an underground two-level island station, with a total length of 208.4 m. The station passes underneath an existing water box culvert, with a clearance of approximately 2.5 m (see Figures 1 and 2). To avoid relocating the box culvert, the station was constructed using open-cut methods at both ends, while the central section was constructed using mechanized excavation. The mechanized excavated section features a single-column double-span structure, measuring 22.6 m by 13.53 m, with a total length of 70 m, as shown in Figure 2. The structure's depth is 20.61 m, with a maximum cover of 7.1 m. The pipe jacking method for metro station construction divides a large space into smaller sections. The station's cross-section was split into two parallel lines: the left and right substructures, as illustrated in Figure 2. Each substructure was constructed sequentially using a super-large rectangular pipe jacking machine with prefabricated segments, maintaining a separation of approximately 5 cm between them. Upon completing the structural conversion, these substructures combined to form a unified metro station space.

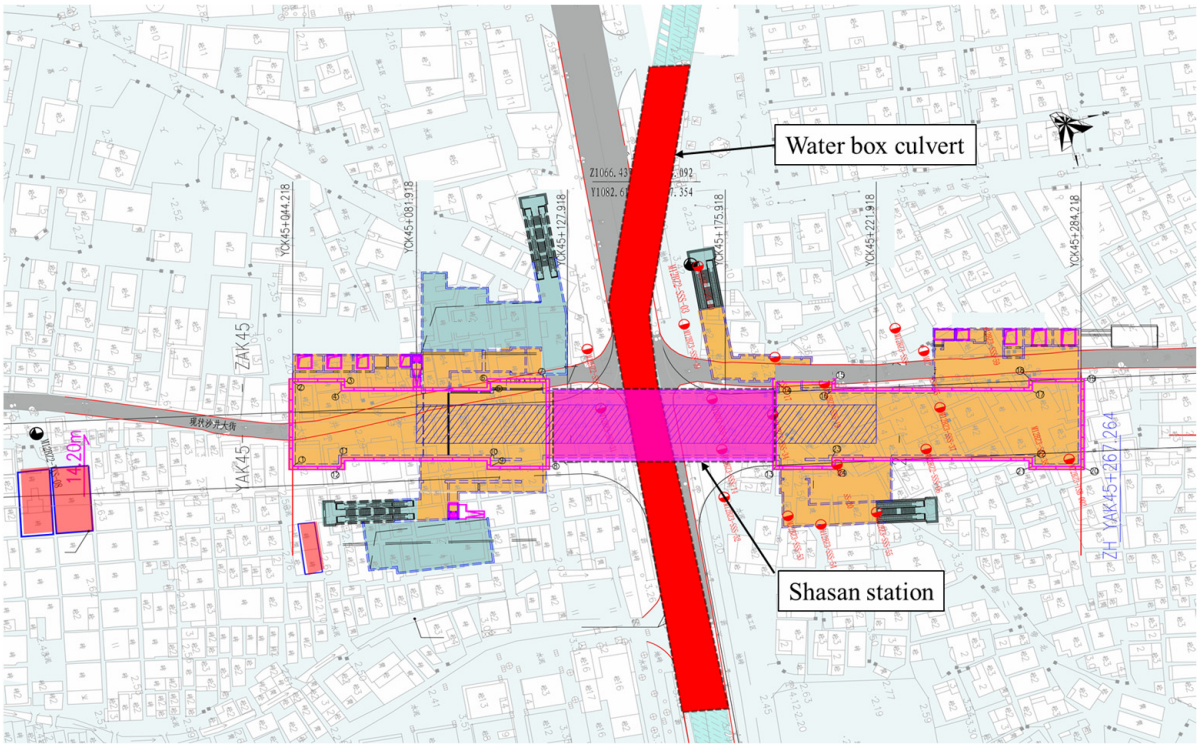

Figure 1. Shasan station general plan.

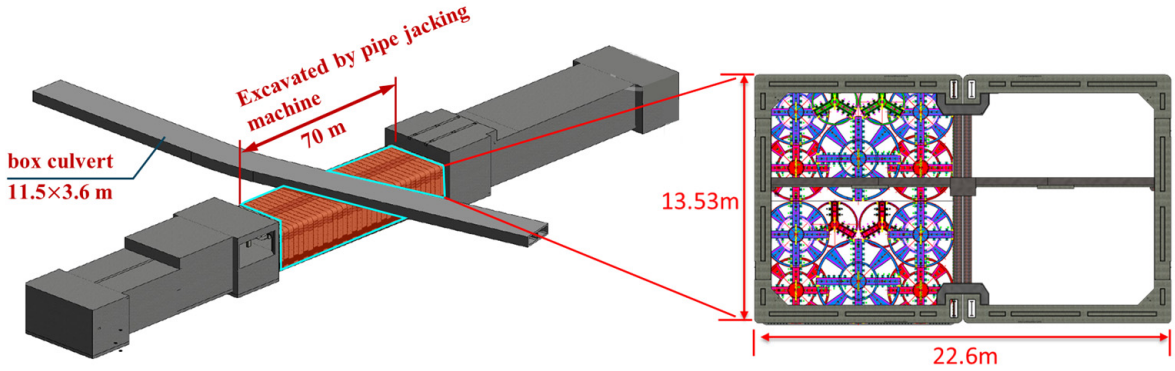

Figure 2. Structural system and mechanical excavation section of the metro station.

2.2. Geological Characteristics

The geological characteristics of the mechanized excavation section at Shasan Station are marked by a horizontally stratified distribution of soil layers. From top to bottom, the exposed strata include Quaternary artificial fill, Quaternary marine-terrestrial silt, Holocene silty clay, and hard plastic sandy clay, underlain by fully to highly weathered granite at the station's base (see Figure 3). The soil parameters are provided in Table 2. The groundwater table is situated at a depth of 0.5 to 2.2 m.

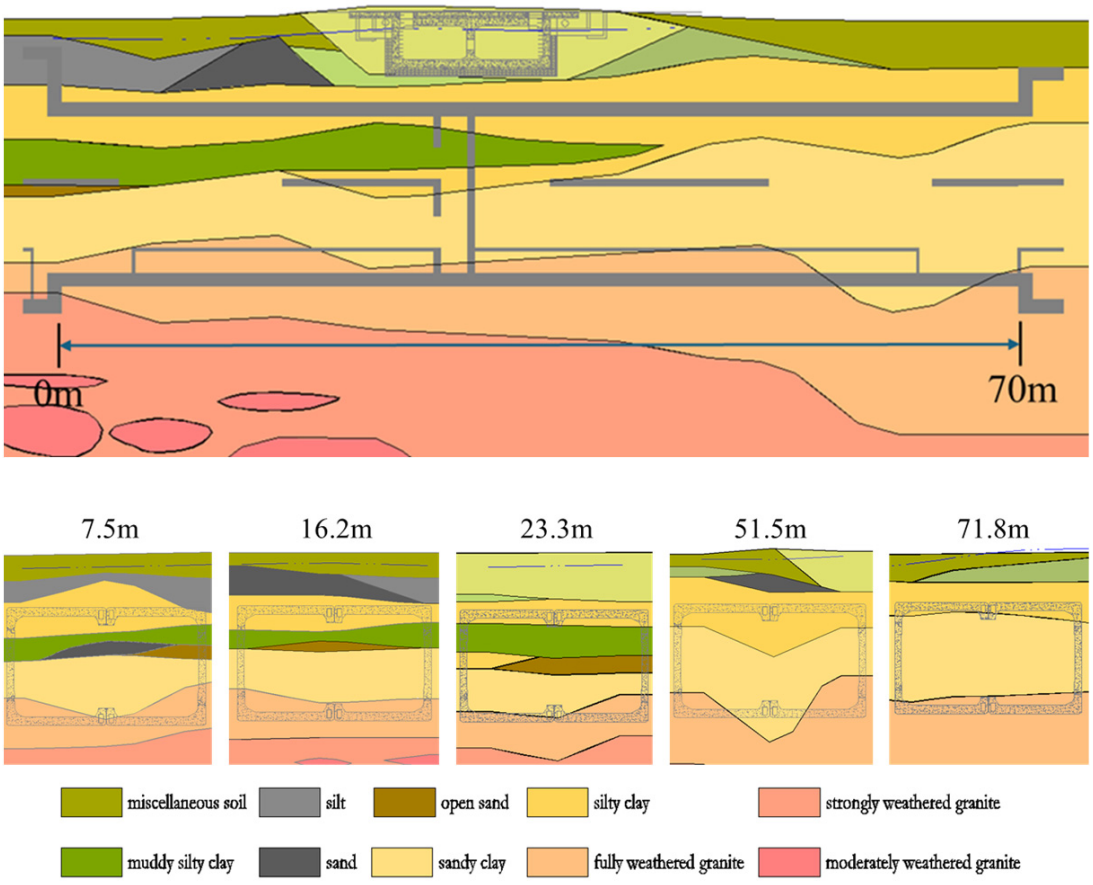

Figure 3. Geological profile and cross-section of mechanical excavation section of metro station.

Table 2. Main soil parameters along the alignment.

Soil Layer	Average Layer Thickness (m)	Elastic Modulus (MPa)	Density (kN/m^3)	Cohesion (kPa)	Internal Friction Angle (°)
Miscellaneous soil	2.4	10.0	17.8	18.0	8.00
Sand	1.9	8.3	19.0	0.0	30.0
Muddy silty clay	2.4	2.5	16.0	10.0	4.0
Silty clay	7.6	13.0	18.8	22.5	12.5
Sandy clay	8.7	35.0	18.5	25.0	22.5
Strongly weathered granite	7.2	70.0	19.0	30.0	25.0

2.3. EPB Rectangular Pipe Jacking Machine

For Shasan Station, a new type of mechanized equipment, the "Dayu Excavation Machine", was developed. This is the world's largest rectangular pipe jacking machine. The tunnel excavated by the rectangular pipe jacking machine has cross-sectional dimensions of 11.275 m in width and 13.53 m in height, with a single-pass excavation area of 153 m^2. This meets the ultra-large section classification standard according to the ITA tunnel section classification criteria (>100 m^2). The machine is composed of two identical EPB TBMs stacked vertically, with design parameters provided in Table 3.

Table 3. Technical parameters of the rectangular pipe jacking machine.

Items	Specification
Model	CTPJ11295 × 13,550
Machine Type	Earth Pressure Balance Rectangular Pipe Jacking Machine
Excavation Size (mm)	11,295 × 13,550
Excavation Configuration	Parallel axis front and rear combination cutterheads
Max Thrust Force (kN)	103,200
Max Steering Force (kN)	160,314
Overall Length (mm)	Approx. 11,900
Cutterhead Count	7 + 7
Model	CTPJ11295 × 13,550
Machine Type	Earth Pressure Balance Rectangular Pipe Jacking Machine
Cutterhead Diameter (mm)	Φ4800 (2), Φ4200 (4), Φ3600 (4), Φ2800 (4)
RPM (r/mi)	0–1.01 (Φ4800) 0~1 (Φ4200) 0~1 (Φ3600 lower) 0~1.1 (Φ3600 upper) 0~1.33 (Φ2800)
Rated Torque (kNm)	2977.7 (Φ4800) 2005 (Φ4200 lower) 1732 (Φ4200 upper) 1732 (Φ3600 lower) 1000 (Φ3600 upper) 695 (Φ2800)
Number of screw conveyors (PCS)	2 + 2
Max Output Capacity (m^3/h)	153
Max Grain Size (mm)	Φ280

Figure 4 illustrates that the rectangular pipe jacking machine is equipped with 14 cutterheads, with those in the upper and lower area of EPB TBM aligned in the same position. A multi-level, parallel axis arrangement of the cutterheads is adopted. The top shield of the pipe jacking machine is extended, with two green-colored cutterheads positioned at the front of the first layer, six cutterheads in the middle layer, and six cutterheads in the bottom layer. This arrangement creates a micro-step form excavation pattern, minimizing

disturbance to the soil above the machine. The cutterheads, varying in diameter, are arranged both front and back, with their excavation areas overlapping, achieving a nearly 90% excavation coverage rate.

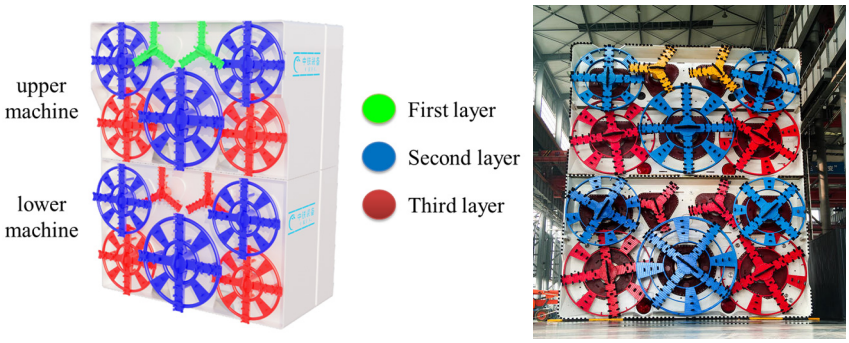

Figure 4. Combined EPB rectangular pipe jacking machine.

The pipe jacking machine excavated a horizontally stratified soil layer, with an excavation height of up to 13.55 m. This led to a wide variety of soil types along the tunnel alignment, as well as significant fluctuations in soil and water pressure. As shown in Figure 4 and Table 3, the equipment is fitted with four different diameters of cutterheads, positioned across different areas of the excavation cross-section. During tunneling, the cutterhead RPM is adjusted based on its diameter and position. The cutterhead design parameters, operational parameters, soil properties, and environmental factors in this project are notably more diverse than in other projects, and the data collected will provide valuable insights for a comprehensive analysis of how these factors influence cutterhead torque.

3. Cutterhead Torque Characteristics

As shown in Figure 2, the rectangular pipe jacking machine progresses in two stages, excavating 70 m to form the main structure of the underground station. Each pipe segment is 2 m wide. After assembling the pipe segments to the fourth ring, the cutterhead contacted the soil and begins excavation. Due to the large excavation cross-sectional area and height, stability at both the launch and reception ends is maintained by reinforcing the soil within an 8 m width at each end, forming an underground wall with enhanced strength and waterproofing properties. Consequently, the thrust required by the machine increases significantly within the reinforced areas, as shown in Figure 5.

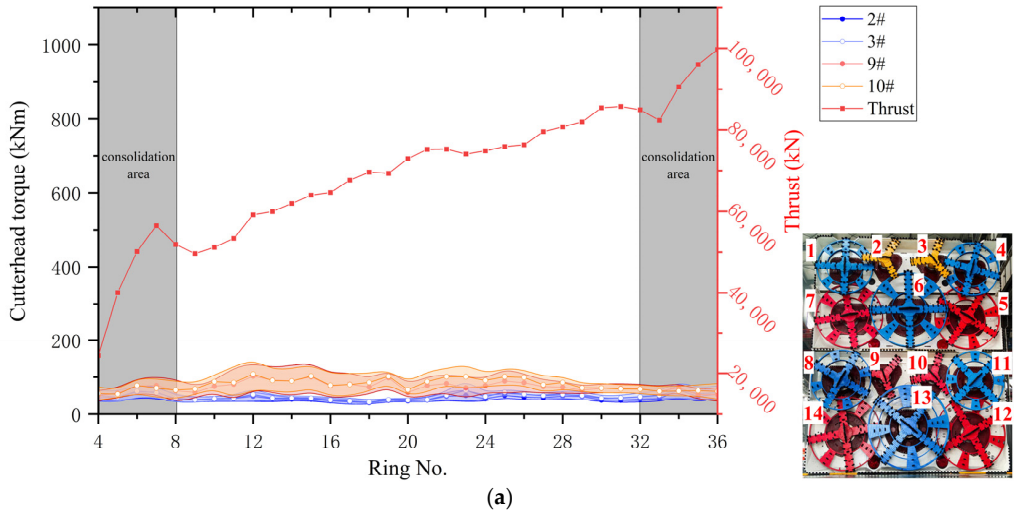

(**a**)

Figure 5. *Cont.*

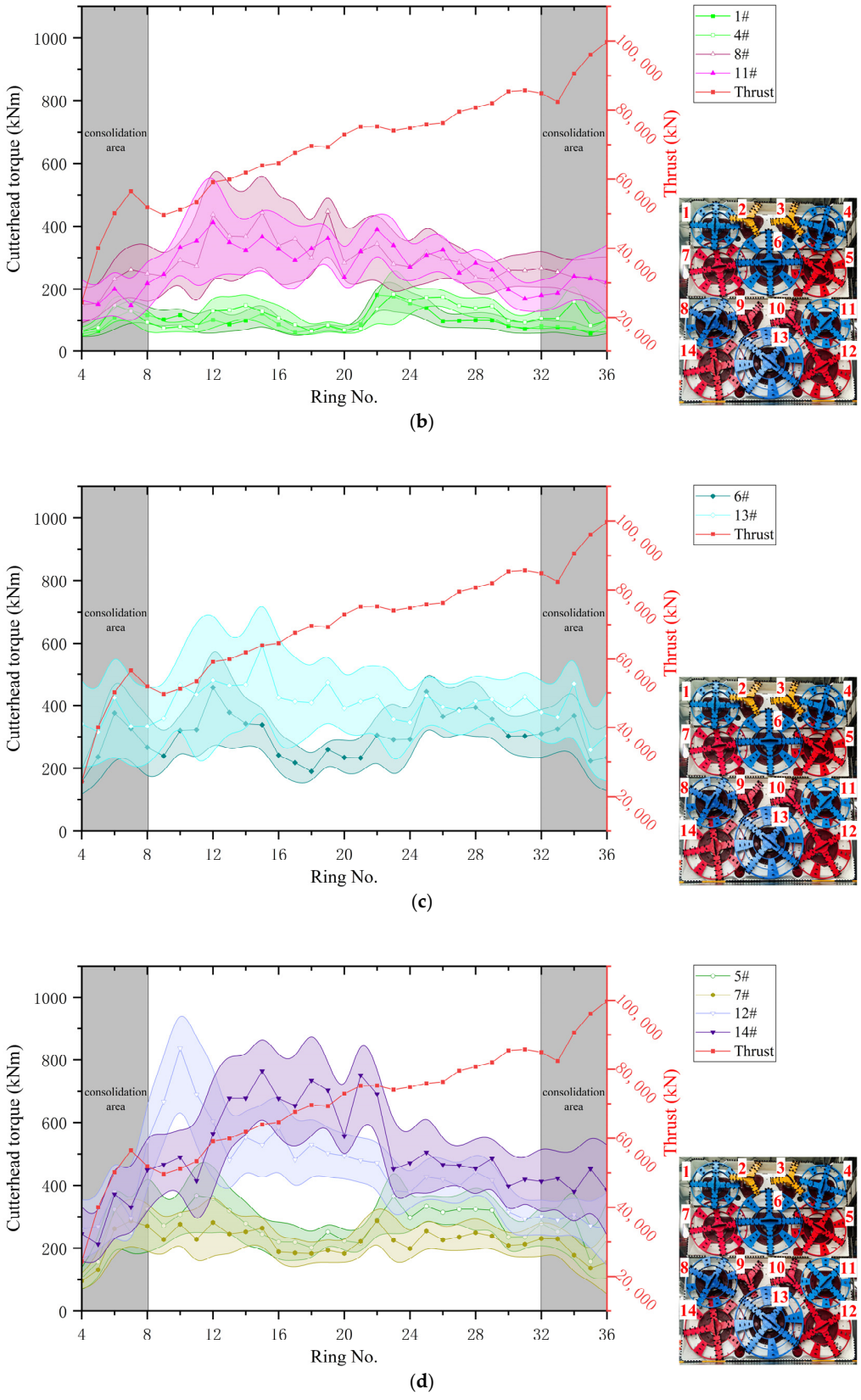

Figure 5. Cutterhead torque distribution. (**a**) Torque distribution of cutterhead 2#, 3#, 9#, 10#; (**b**) torque distribution of cutterhead 1#, 4#, 8#, 11#; (**c**) torque distribution of cutterhead 6#, 13#; (**d**) torque distribution of cutterhead 5#, 7#, 12#, 14#.

3.1. Torque Characteristics of Different Cutterheads

Taking the left line tunneling as an example, Figure 5 illustrates the torque of each cutterhead during the excavation process, with the cutterheads numbered from top to bottom according to their position. To facilitate a clear analysis, comparisons were made between the cutterheads of the same diameter located at different heights. Figure 5a–d present the average torque and total thrust for cutterheads with diameters of 2800 mm (2#, 3#, 9#, 10#), 3600 mm (1#, 4#, 8#, 11#), 4800 mm (6#, 13#), and 4200 mm (5#, 7#, 12#, 14#) for each ring. The scale on the axes is consistent across all figures. The light-color areas represent the standard deviation of the torque for each ring, with a larger range indicating greater fluctuations in torque values.

The figures clearly show that, for cutterheads of the same diameter, the torque of the lower cutterheads is significantly higher than that of the upper ones, with a wider range of torque fluctuations. For instance, in Figure 5a, cutterheads 2#, 3#, 9#, and 10# all have a diameter of 2800 mm. The average torques for cutterheads 2# and 3# are 41.34 kNm and 45 kNm, with standard deviations of 7.08 and 8.64, respectively. Meanwhile, cutterheads 9# and 10# exhibit torques of 77.78 kNm and 85.05 kNm, with standard deviations of 24.62 and 23.07. For the largest diameter cutterheads (4800 mm), the torques for 6# and 13# are 311.47 kNm and 419.38 kNm, with standard deviations of 76.70 and 119.74. These results indicate that the operating conditions of the lower cutterheads are less stable, which can be attributed to two main factors.

Firstly, due to the depth, the deeper cutterheads are subjected to higher soil and water pressures, leading to greater frictional resistance during the cutting process. As shown in Figure 6, the pressure in the cutterhead's soil chamber lies between the static earth pressure and the Rankine passive earth pressure, approximately 2.5 times closer to the static earth pressure. Secondly, there are variations in the properties of the excavated soil. According to the stratigraphic distribution, the upper excavated soil primarily consists of silty clay and muddy clay (represented by the dark gray soil in the middle of the muck bucket in Figure 7), while the deeper excavated soil comprises sandy clay and fully weathered granite (shown as yellowish-brown soil on both sides of the muck bucket in Figure 7). Soil properties, such as shear strength and liquid and plastic limits, can influence the operational parameters of the cutterhead [21]. The specific effects will be analyzed in the following sections of this paper.

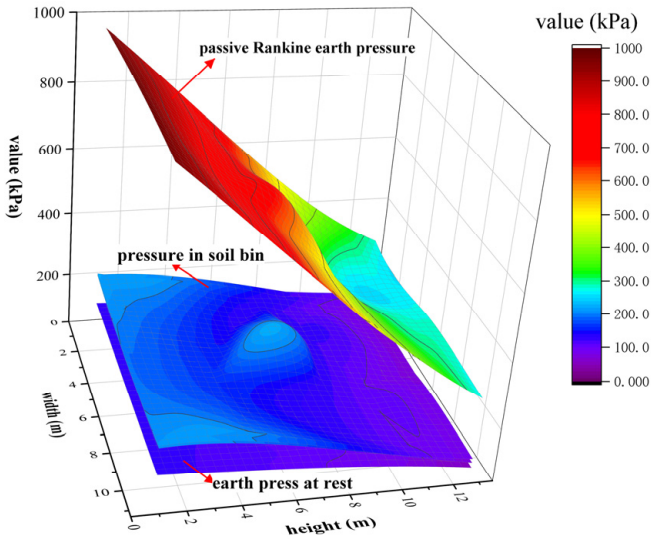

Figure 6. Pressure distribution in the soil chamber of pipe jacking machine.

Figure 7. Muck transport.

Under normal circumstances, at the same depth, the torque of the cutterhead increases significantly as the diameter of the cutterhead increases. For example, the average torque of cutterhead #6 (4800 mm) is 311.47 kNm, compared to 230.79 kNm for cutterhead #7 (4200 mm). However, as shown in Figure 5c,d, between the 9th and 23rd ring, the torque of cutterheads #12 and #14, located at the outermost edge of the pipe jacking machine, is approximately 30% to 40% higher than that of cutterhead #13, which is positioned centrally. This difference is primarily due to the uneven weathering of the bedrock at the bottom of the excavation, which is characterized by significant undulations in the weathering interface and isolated boulders caused by uneven weathering. Furthermore, the consolidation of muck in the blind area at the lower edge of the cutterhead leads to abnormal local soil pressure within the soil chamber, which also affects the cutterhead torque, as shown in Figure 8.

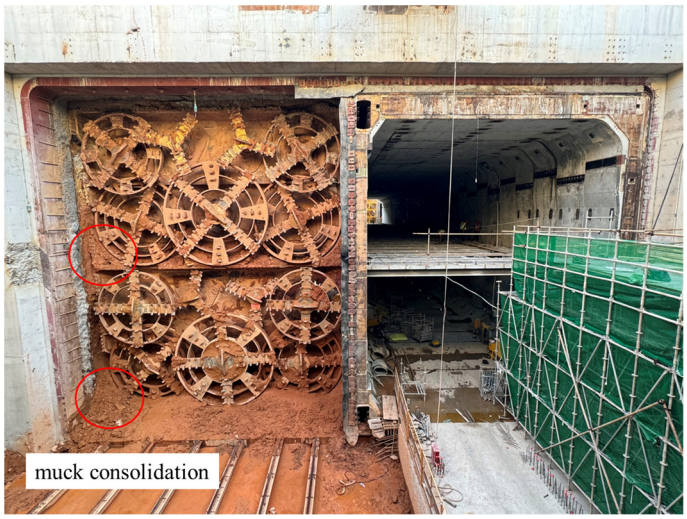

Figure 8. The consolidation of muck in the blind area.

3.2. Torque Characteristics During Excavation Stages

The muck bucket of the rectangular composite tunneling machine at Shasan Station has a capacity of approximately 24 m^3. Consequently, after tunneling about 120 to 140 mm, the muck fills the muck bucket and the machine stops and discharges the muck. This cycle process is referred to as a tunneling progression. The previous section analyzed the distribution characteristics of the torque for different cutterheads. Now, the microscopic

variations in parameters during each tunneling progression are examined. Figure 9 records the tunneling parameters for four cycle processes during the 21st ring of the left line, including the torque and RPM of cutterheads 5# (upper 4200 mm), 12# (lower 4200 mm), and 13# (lower 4800 mm), as well as the penetration rate and thrust of the machine.

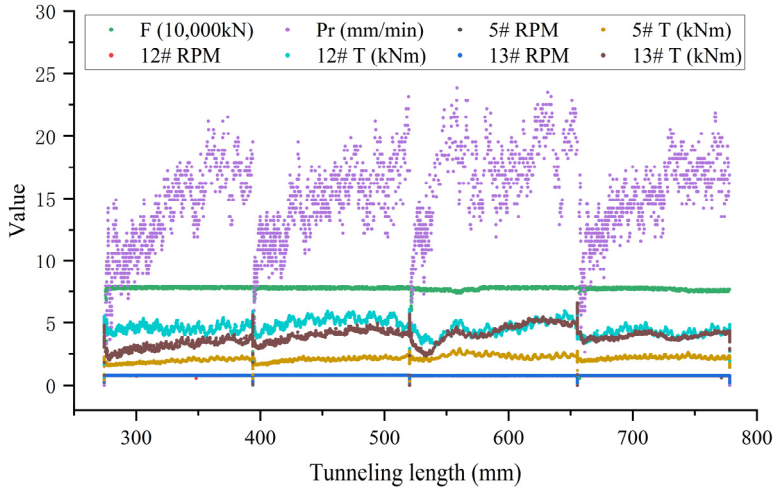

Figure 9. Operational parameters of several tunneling process cycles.

The figure shows a sudden increase in torque after each start of the tunneling progression. This phenomenon is primarily due to the consolidation of the soil surrounding the cutterhead, resulting in the dissipation of pore water pressure in the soil. As a result, the effective stress and frictional resistance acting on the cutterhead increase. Based on the characteristics of the tunneling parameters, each excavation cycle can be categorized into the following typical stages:

i. Start-Up Stage: The cutterhead starts rotating and quickly reaches its rated RPM, resulting in a sharp increase in torque that is significantly higher than during normal tunneling conditions. This stage lasts a very short time, generally around 1 min.

ii. Loading Stage: The phase begins as the pipe jacking machine starts pushing forward. With the injection of foam stabilizer, the cutterhead torque gradually decreases to normal levels, while the thrust reaches its peak. The penetration rate rises from 10 mm/min to 20 mm/min, with the cutterhead torque fluctuating within a defined range. This phase typically lasts for 4 to 5 min.

iii: Stabilization Stage: During this phase, the thrust, penetration rate, and RPM remain stable. The torque relationship $T_{12\#} > T_{13\#} > T_{5\#}$ aligns with previous observations. This phase is governed by the penetration rate and generally lasts for 6 to 7 min.

iv: Stop Stage: Once the muck has filled the muck bucket, the pipe jacking machine ceases its pushing forward. The cutterhead gradually reduces its rational speed, and the retracting device is fixed in place to maintain soil chamber pressure.

During the tunneling process, the cutterhead RPM and the thrust remain relatively constant, while the penetration rate and cutterhead torque exhibit significant variations. For approximately one-third to two-thirds of each tunneling cycle, the penetration rate increases during a rising phase before stabilizing. The operational parameters during the tunneling with a rectangular pipe jacking machine differ significantly from those of hard rock TBMs. Unlike rock mass, which has high strength and a structured behavior, the soil is less cohesive and more porous. Consequently, the loading phase in pipe jacking machines is less pronounced compared to hard rock excavation. In soft ground, the torque serves as a more effective indicator of real-time excavation conditions and soil quality than thrust force.

4. Cutterhead Torque Prediction Model

The analysis of cutterhead torque distribution patterns revealed that torque is influenced by multiple factors, including design specifications, geological and environmental conditions, and operational parameters. During the tunneling beneath the box culvert (14th–20th rings), the machine operated a full-chamber state to maintain the tunnel face stability and minimize surrounding ground disturbance. Under these conditions, all cutterheads operated with their normal operating conditions. To account for the characteristics of the excavated grounds and the state of the tunneling process, data from the 14th to the 20th rings of both lines were selected for analysis. This dataset reflects stable operational conditions and provides a reliable basis for evaluating torque behavior under uniform working scenarios.

4.1. Database Establishment

The soil's mechanical parameters in the research area have been determined through laboratory tests and preliminary geotechnical investigations. Operational parameters were extracted from the automatic recording system of a pipe jacking machine. Based on these data, a comprehensive database was established, encompassing soil parameters (shear strength (τ), consistency index (I_c)), cutterhead design parameters (diameter (D)), and operational parameters (RPM, penetration rate (PR), solid chamber pressure (P)). The database comprises 207,074 datasets collected over a 28-meter section corresponding to the 14th–20th rings of both tunnel lines.

4.2. Univariate Analysis

Regression analysis was conducted to assess the correlation and variation trends between the cutterhead torque (T) and various factors. This analysis provides a foundational basis for the subsequent development of the EPB cutterhead torque prediction model. Figure 10 illustrates the correlation of the cutterhead torque with each factor that informs the model.

Among the various factors influencing T, the D and RPM show the most significant correlation, with a coefficient of determination (R^2) of 0.64. The cutterhead D determines the area of soil being cut and the contact area with the soil, making it a key determinant of cutterhead T. Previous studies have primarily focused on the frictional resistance between the cutterhead and the surrounding soil during tunneling, which depends on the friction coefficient and contact area. The cutterhead RPM is another critical factor, although this is rarely overlooked in discussions. The theory suggests that a higher cutterhead speed increases resistance and demands greater torque. However, Figure 10b reveals an inverse relationship, with the torque decreasing as the RPM increases.

Figures 9 and 11a show that the cutterhead RPM rapidly stabilizes at its rated speed shortly after starting, making it well suitable for operation in homogeneous soft soil strata. This rated RPM is related to the cutterhead D. As the D increases, the rated RPM decreases. This trend is further illustrated by the data distribution in Figure 11b. Therefore, the cutterhead RPM in this study is primarily considered as a design parameter. Here, the RPM refers to the rated RPM of the cutterhead, denoted as RPM_{rated}. To analyse the relationship between different RPM and T, a more detailed categorization of the cutterhead RPM distribution in the database is necessary.

Figure 10c,d demonstrate a positive correlation between T and both P and τ. P represents the effective stress between the cutterhead and the surrounding soil. Meanwhile, τ directly affects the ease of soil cutting and mixing.

Soil moisture content significantly affects its plastic state. Higher moisture content causes the soil to transition from a solid to a plastic state and, ultimately, to a fluid state. Hollmann and Thewes (2013) [30] introduced the I_c to assess the impact of clay properties on mechanical excavation, as depicted in Figure 12. The calculation formula for I_c is shown in Equation (1), where W_L represents the liquid limit, W_n denotes the natural moisture content, and I_P is the plasticity index. Avunduk and Copur (2018) [21] observed that higher

I_c values correspond to increased cutterhead torque, a trend also evident in Figure 10e. As the consistency index increases, viscous soil becomes softer and stickier, making it prone to adhering to the cutterhead's metal surface, causing blockages and increased torque.

$$I_C = (W_L - W_n)/I_P \quad (1)$$

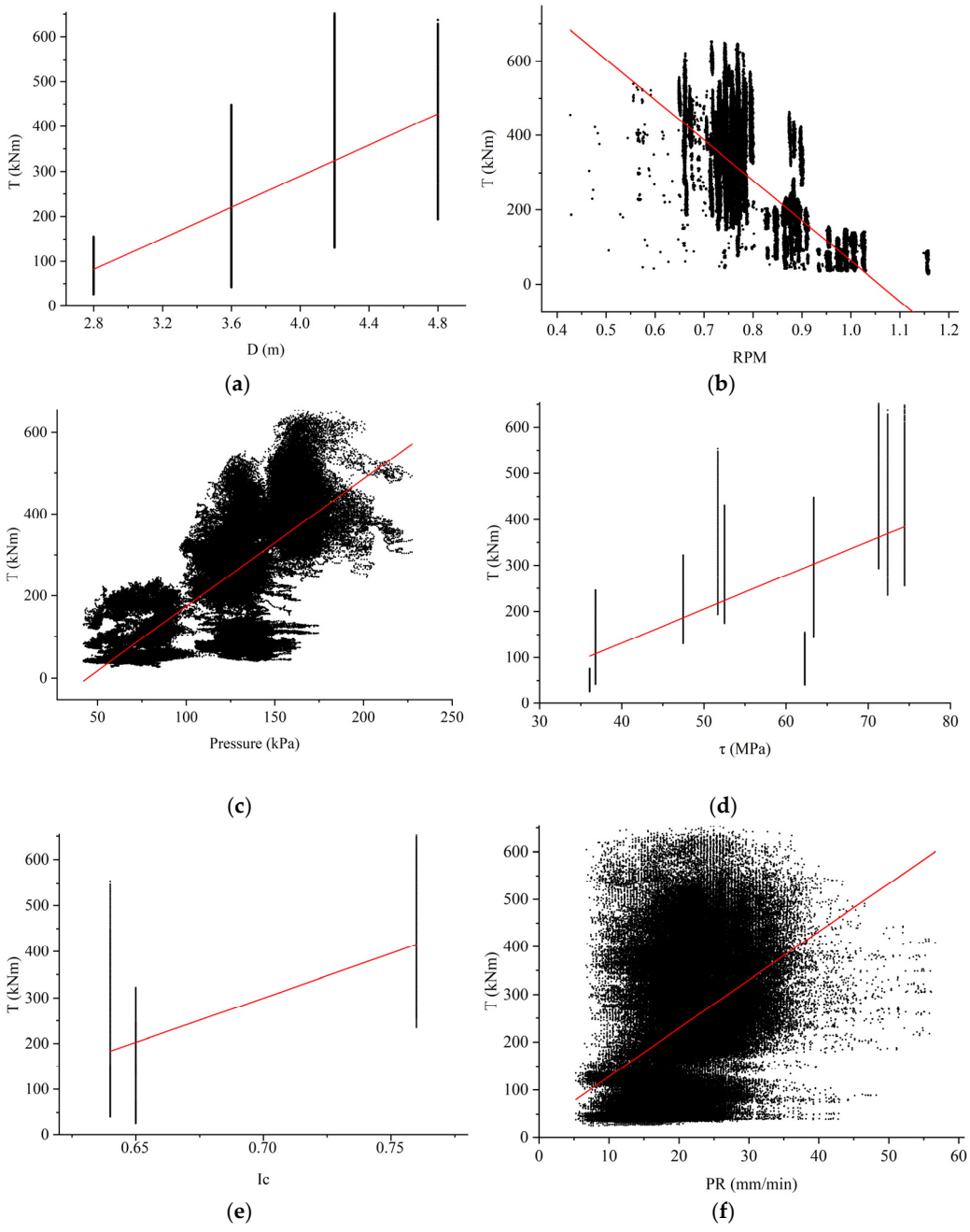

Figure 10. The correlation between cutterhead torque and various factors. (**a**) T vs. D (R^2 = 0.64); (**b**) T vs. RPM (R^2 = 0.64); (**c**) T vs. P (R^2 = 0.52); (**d**) T vs. τ (R^2 = 0.45); (**e**) T vs. I_c (R^2 = 0.38); (**f**) T vs. PR (R^2 = 0.15).

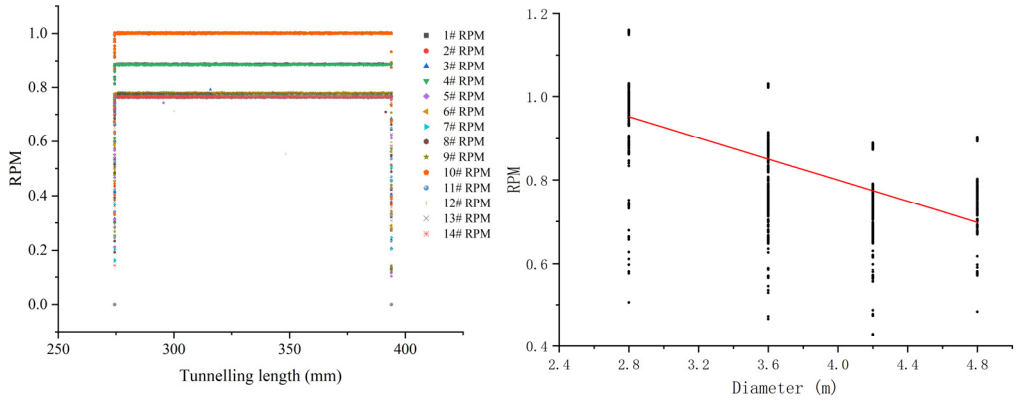

Figure 11. Distribution characteristics of cutterhead RPM. (**a**) Distribution of each cutterhead RPM (data same as Figure 7); (**b**) relationship between D and RPM.

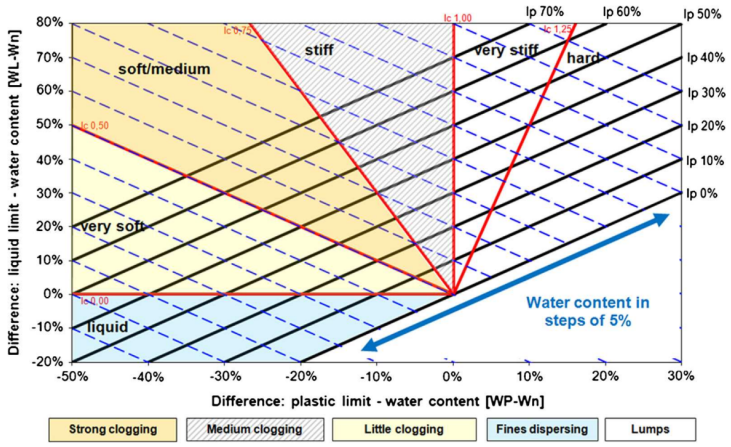

Figure 12. Clogging potentials of the soil with the influence of water content (after [30]).

Figure 10f reveals a weak correlation between the *PR* and *T*, with an R^2 of just 0.15. The *PR* is primarily determined by the thrust of the push cylinders, but it also depends on complex factors such as the interaction between the shield, the ring, and the surrounding soil, as well as the soil discharge conditions. Consequently, the factors influencing the *PR* are multifaceted and challenging to isolate.

4.3. Multiple Linear Regression Analysis

A correlation analysis of the factors influencing cutterhead *T* was used to establish functional relationships between these factors and the *T*. The selected independent variables were *D*, RPM_{rated}, *P*, τ, and I_c, with cutterhead *T* as the dependent variable. Multiple regression analysis was conducted using SPSS statistical analysis software to fit the torque calculation formula.

The correlation analysis between the independent variables and the dependent variable revealed that all parameters exhibit a good linear relationship with *T*, demonstrating high correlation and clear physical significance. Therefore, multiple linear regression analysis was conducted using a stepwise regression input method. This method involves recalculating the contribution of already included independent variables after adding each new variable to assess their ongoing relevance to the equation. Variables are alternately added or removed based on their significance, until no further changes can be made. The detailed steps are as follows, and the flowchart is shown in Figure 13.

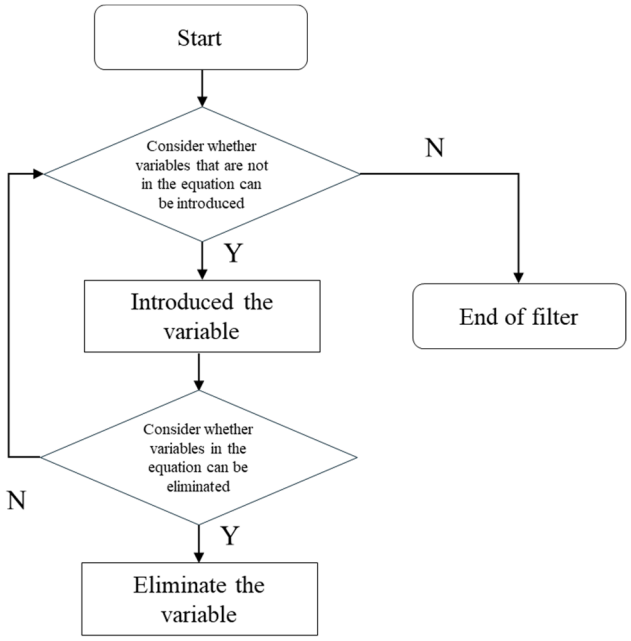

Figure 13. The basic steps of the stepwise regression input method.

Step 1: Establish a unary regression model for p independent variables $X_1, X_2, \cdots, X_P$, and dependent variable Y, respectively.

$$Y = \beta_0 + \beta_i X_i + \epsilon, i = 1, \cdots, p \tag{2}$$

The calculation of variable X_1 corresponding regression coefficients of F the value of the test statistics to $F_1^{(1)}, F_2^{(1)}, \cdots, F_P^{(1)}$, take the maximum value $F_{i_1}^{(1)}$.

$$F_{i_1}^{(1)} = max\left\{F_1^{(1)}, F_2^{(1)}, \cdots, F_P^{(1)}\right\} \tag{3}$$

Compare $F_{i_1}^{(1)}$ with the threshold $F^{(1)}$ at a given significance level α, and if the $F_{i_1}^{(1)} > F^{(1)}$, introduce X_{i_1} into the regression model and add it to the set of selected variables I_1.

Step 2: The binary regression model of dependent variable Y and independent variable subset $\left\{X_{i_1}, X_1\right\}, \cdots \left\{X_{i_1}, X_{i_{1-1}}\right\}, \left\{X_{i_1}, X_{i_{1+1}}\right\}, \cdots, \left\{X_{i_1}, X_P\right\}$ is established (that is, the regressors of this regression model are binary), with a total of p−1. Compute the F-statistic for each variable, denoted as $F_k^{(2)}$ (k is not included in I_1), the largest of which is denoted as $F_{i_2}^{(2)}$, and the corresponding independent variable foot is denoted as i_2, that is

$$F_{i_2}^{(2)} = max\left\{F_1^{(2)}, \cdots, F_{i_1-1}^{(2)}, F_{i_1+1}^{(2)}, \cdots F_P^{(2)}\right\} \tag{4}$$

Compare $F_{i_2}^{(1)}$ with the threshold $F^{(2)}$ at a significance of α, and if the $F_{i_2}^{(1)} > F^{(2)}$, the variable X_{i_2} is introduced into regression model. Otherwise, terminate the variable introduction process.

Step 3: Repeat Step 2 by adding one independent variable at a time to the model, using subsets $\left\{X_{i_1}, X_{i_2}, X_k\right\}$, until no additional variables meet the inclusion criteria.

This method ensures a logical selection of independent variables, minimizing the influence of statistically insignificant factors on the final regression equation. Variables causing multicollinearity can be identified and excluded. Following stepwise regression, the remaining explanatory variables are both significant and free from severe multicollinearity.

The analysis revealed that none of the independent variables were excluded, indicating their significant impact on the cutterhead T. By systematically incorporating the various influencing factors, the resulting fitted equations were derived and are presented in Table 4.

Table 4. The prediction model based on the stepwise regression input method.

Model	R^2	F	Sig.
$T = 172.78D - 401.55$	0.64	363,434.23	<0.0001
$T = 137.01D + 4.67\tau - 524.72$	0.79	398,073.52	<0.0001
$T = 90.82D + 4.13\tau - 395.41RPM_{rated} + 7.07$	0.82	318,955.03	<0.0001
$T = 77.57D + 3.44\tau - 444.79RPM_{rated} + 367.36I_c - 112.65$	0.83	251,018.15	<0.0001
$T = 75.61D + 3.09\tau - 444.29RPM_{rated} + 368.66I_c + 16.35P - 104.96$	0.83	201,097.33	<0.0001

The table above indicates that as more variables are added to the model, the adjusted R^2 values show an upward trend. When the independent variables, including D, τ, and RPM_{rated}, are considered together, the adjusted R-squared values for all models exceed 0.8. The resulting regression equation is robust and demonstrates strong explanatory power for the dependent variable.

The F-values and significance coefficients for all the models confirmed the statistical validity of the regression model, indicating that the inclusion of the independent variables improves the model's predictive ability. The multicollinearity analysis shows that a tolerance value above 0.1 and a variance inflation factor (VIF) below 10 indicate no multicollinearity between the independent variables, particularly between the cutterhead diameter and RPM. Therefore, it is reasonable to assume that multicollinearity among the independent variables is not present in this analysis.

Considering all independent variables, the prediction model of the cutterhead torque is as follows:

$$T = 75.61D + 3.09\tau - 444.29RPM_{rated} + 368.66I_c + 16.35P - 104.96 \quad (5)$$

The standardized coefficients for the independent variables D, τ, RPM_{rated}, I_c, and P are 0.35, 0.28, −0.33, 0.12, and 0.04, respectively. These coefficients indicate that the various factors influencing the cutterhead torque, ranked from highest to lowest, are as follows: cutterhead diameter (D), cutterhead-rated RPM (RPM_{rated}), soil shear strength (τ), consistency index (I_c), and chamber pressure (P). A comparison of the predicted and actual cutterhead torque values is illustrated in Figure 14.

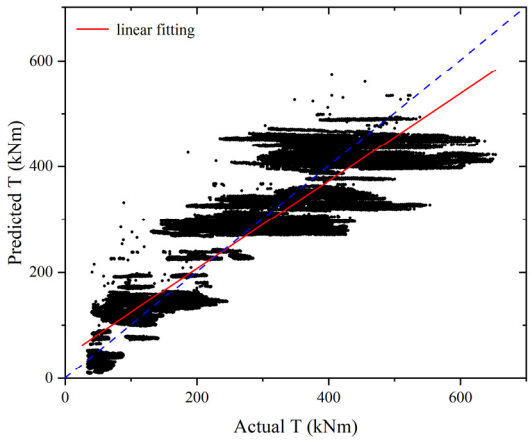

Figure 14. Comparison between the predicted and actual values of cutter torque.

4.4. Neural Network Prediction Using the Levenberg–Marquardt Algorithm

Artificial neural networks (ANNs) can model the relationship between input and output without requiring a predefined mathematical equation. The Levenberg–Marquardt

(L-M) algorithm, used in nonlinear neural network learning, integrates the Gauss–Newton method with the steepest descent method. By adaptively adjusting the damping factor, the algorithm achieves stable and reliable solutions, characterized by a higher rate of iterative convergence. The L-M algorithm's ability to dynamically transition between gradient descent and Gauss–Newton approaches ensures a robust and efficient optimization process. It effectively balances global stability with local convergence speed, making it one of the most reliable methods for nonlinear least squares problems.

This study utilized MATLAB's built-in neural network toolbox to predict the cutterhead torque of the rectangular tunneling machine. The data samples used for this analysis were identical to those employed for the multiple linear regression fitting. The independent variables—D, RPM_{rated}, P, τ, and I_c—were set as input parameters, while the cutterhead torque (T) was designated as the output parameter. To avoid overfitting, the dataset was divided into 70% for training, 15% for validation, and 15% for testing. The training algorithm employed the L-M algorithm method with a neural network structure consisting of 10 hidden layers. The neural network structure is illustrated in Figure 15.

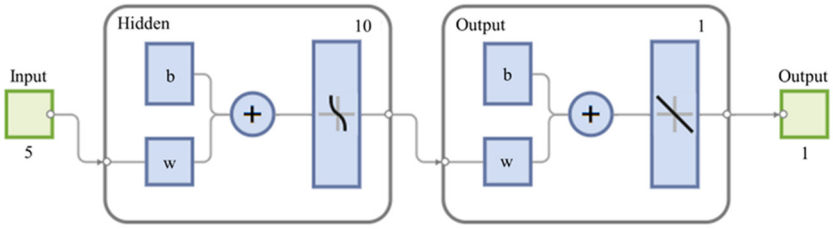

Figure 15. The neural network structure.

The results of the prediction model are shown in Figure 16, featuring regression plots for the training set, validation set, test set, as well as the combined dataset. The model achieved a correlation coefficient (R) exceeding 0.95 and an R^2 value exceeding 0.91, indicating that the model has a significant predictive effect and excellent data interpretability. These results confirm that neural networks are highly effective in predicting cutterhead torque.

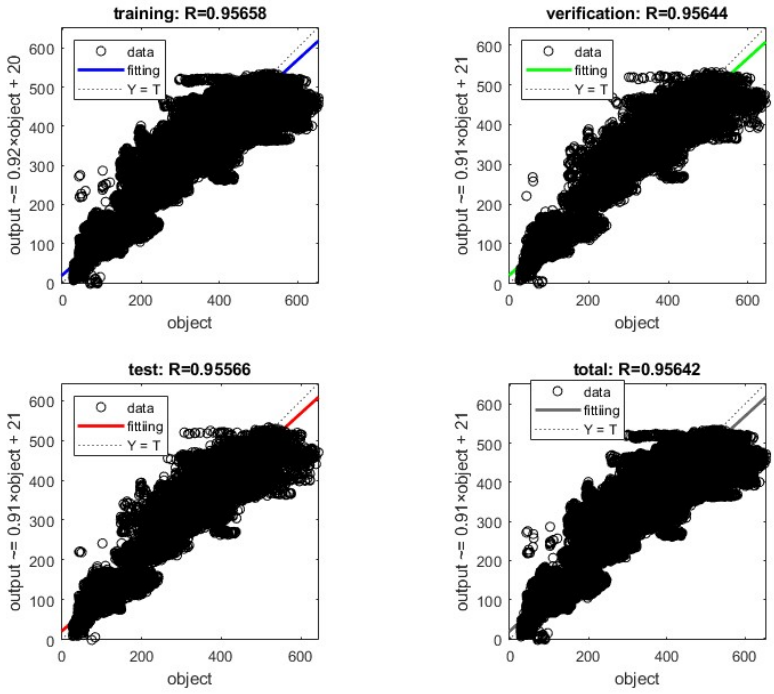

Figure 16. The fitting result of the prediction model with different datasets.

Figure 17 presents the error histogram, illustrating the discrepancies between the predicted and target outputs. The histogram shows that errors for the training set, validation set, and test set are predominantly clustered around zero, confirming the reliability of this model.

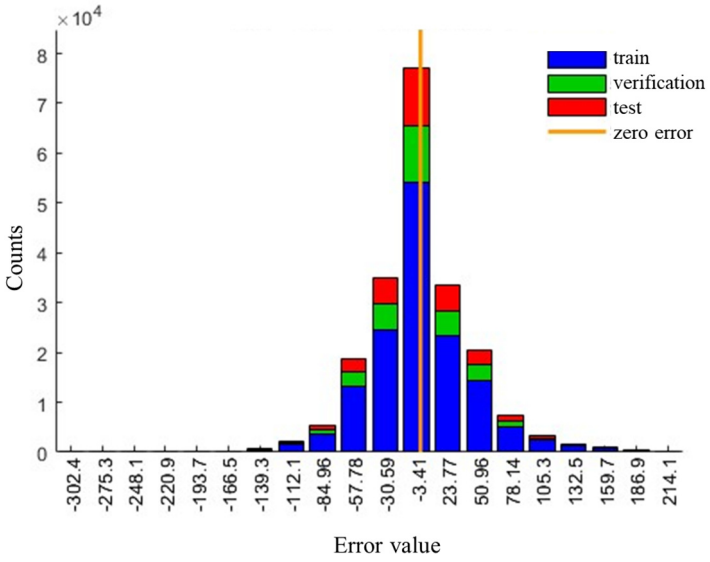

Figure 17. Distribution of error histogram.

5. Determination and Evaluation of Prediction Models

Developing a prediction model is central to quantitative forecasting, as it identifies inherent patterns and serves as the foundation for predicting future values. The effectiveness of a prediction model can be assessed using the following several key principles:

Sound theoretical foundation: a forecasting model must rely on a robust theoretical framework that captures the underlying patterns and logical relationships of real-world phenomena. Statistical reliability: the model must undergo rigorous statistical testing to ensure stability, reliability, and the ability to capture data trends accurately. Forecasting accuracy: a reliable model should consistently provide accurate and dependable predictions of future trends or outcomes. Ease of application: the model should be straightforward, user-friendly, and practical for real-world use.

Beyond accuracy, the logical coherence and physical relevance of the model are crucial, as they determine its practical applicability.

Comparisons show that the neural network algorithm provides more accurate predictions, attributed to its strong modeling capability and adaptability. However, the internal workings of the neural network, such as weight adjustments and structure changes, are difficult to interpret, limiting its ability to explain the physical relationships and significance between the independent and dependent variables. Consequently, the model's interpretability is relatively limited.

A satisfactory predictive model was also developed through multiple linear regression analysis (R^2 = 0.83), which explicitly reflects the relationships and weights of various parameters influencing cutterhead torque in the prediction formula. Considering all factors, the multiple linear regression prediction model (Equation (5)) was selected as the preferred prediction model for the cutterhead torque of the EPB TBMs.

Predicted cutterhead torque values from this model and previous prediction models in Table 1 were compared with actual torque measurements, as shown in Figure 18. The model proposed by Shi et al. (2011) [14] did not consider the cutting torque, due to its influence on cutterhead torque being negligible. Prior theoretical and empirical models overestimate the actual cutterhead torque by approximately 170% to 370%, indicating a considerable discrepancy. Additionally, discrepancies grow with increasing torque values

or cutterhead diameters, reaching up to 1700%, consistent with findings by Zhang et al. (2014) [24].

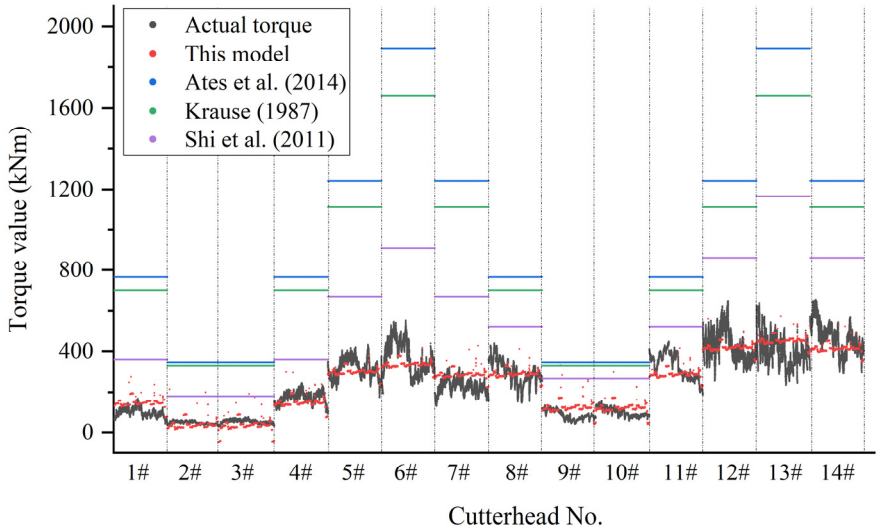

Figure 18. Comparison of prediction effect of different cutterhead torque prediction models (Ates et al. (2014) [4], Krause (1987) [20], Shi et al. (2011) [14]).

The main reason for these discrepancies is that most prior empirical models focused on the cutterhead's design torque during manufacturing, incorporating substantial safety margins to accommodate diverse ground conditions and special operational scenarios encountered during tunneling. Additionally, these theoretical and empirical models often lack comprehensive consideration of the influencing factors, leading to reduced prediction accuracy when dealing with variations in cutterhead design parameters, soil properties, or environmental conditions.

In contrast, the predictions from this model closely align with actual torque values, with an average deviation of about 5% above the actual measurements. This indicates the model's high accuracy in considering factors such as the cutterhead diameter, soil properties, and different burial depths. Therefore, the model provides a reliable foundation for predicting cutterhead torque in EPB TBM and pipe jacking machine tunneling in soil strata.

6. Conclusions

The Shasan Station project of Shenzhen Metro Line 12 employed an ultra-large section rectangular EPB pipe jacking machine for metro station construction. The data collected from the project contained abundant information on cutterhead design, operational parameters, soil properties, and environmental factors. Analysis of the operational data from the pipe jacking machine tunneling process revealed the distribution characteristics of cutterhead torque, highlighting the significant impact of cutterhead diameter and excavation depth.

A database incorporating design, experimental, and field data was established to analyze the correlation between various factors and cutterhead torque. Empirical formulas incorporating various influencing factors were developed using stepwise regression and the L-M algorithm neural network. Considering both interpretability and accuracy, the EPB cutterhead torque prediction model was finalized. The model accounted for multiple influencing factors and demonstrated better predictive results compared to traditional theoretical and empirical models. The factors influencing cutterhead torque, ranked by their impact from highest to lowest, are as follows: cutterhead diameter, cutterhead-rated RPM, soil shear strength, consistency index, and soil chamber pressure. The model is highly

suitable for predicting cutterhead torque in EPB TBM or pipe jacking machine operations in soft ground, providing valuable support for construction activities.

However, the limited sample size in this study's database suggests that additional engineering data are needed to enhance its applicability and accuracy. Moreover, the constrained RPM data distribution limits the model's ability to effectively explain its relationship with cutterhead torque. To address this, a larger dataset encompassing diverse cutterhead rotation speeds is essential to enhance data composition and distribution for better torque predictions.

Author Contributions: Conceptualization, B.S. and Q.G.; methodology, J.L.; software, J.L.; validation, W.L. and W.Z.; investigation, T.S.; resources, Y.L.; writing—original draft preparation, J.L.; writing—review and editing, Q.G. and J.L.; funding acquisition, B.S. and W.L. All authors have read and agreed to the published version of the manuscript.

Funding: This research was funded by the Key Technologies R&D Program of Guangdong Province, grant number 2019B111105001.

Data Availability Statement: The raw data supporting the conclusions of this article will be made available by the authors upon request.

Conflicts of Interest: The authors declare no conflicts of interest.

References

1. Wang, L.; Gong, G.; Shi, H.; Yang, H. A new calculation model of cutterhead torque and investigation of its influencing factors. *Sci. China Technol. Sci.* **2012**, *55*, 1581–1588. [CrossRef]
2. Li, X.; Wu, L.J.; Wang, Y.J.; Li, J.H. Rock fragmentation indexes reflecting rock mass quality based on real-time data of TBM tunnelling. *Sci. Rep.* **2023**, *13*, 10420. [CrossRef] [PubMed]
3. Maidl, B.; Herrenknecht, M.; Maidl, U.; Wehrmeyer, G. *Mechanised Shield Tunnelling*; John Wiley & Sons: Hoboken, NJ, USA, 2013.
4. Ates, U.; Bilgin, N.; Copur, H. Estimating torque, thrust and other design parameters of different type TBMs with some criticism to TBMs used in Turkish tunneling projects. *Tunn. Undergr. Space Technol.* **2014**, *40*, 46–63. [CrossRef]
5. Bruland, A. Hard Rock Tunnel Boring. Ph.D. Thesis, Norwegian University of Science and Technology, Trondheim, Norway, 1998.
6. Rostami, J.; Ozdemir, L. A new model for performance prediction of hard rock TBMs. In Proceedings of the 1993 Rapid Excavation and Tunneling Conference, Boston, MA, USA, 13–17 June 1993.
7. Cigla, M.; Ozdemir, L. Computer modeling for improved production of mechanical excavators. In Proceedings of the 2000 SME Annual Meeting, Salt Lake City, UT, USA, 28 February–1 March 2000.
8. Yi An, Zhuohan Li, Changzhi Wu, Huosheng Hu, Cheng Shao, Bo Li. Earth pressure field modeling for tunnel face stability evaluation of EPB shield machines based on optimization solution. *Discret. Contin. Dyn. Syst.—S* **2020**, *13*, 1721–1741.
9. Naghadehi, M.Z.; Samaei, M.; Ranjbarnia, M.; Nourani, V. State-of-the-art predictive modeling of TBM performance in changing geological conditions through gene expression programming. *Measurement* **2018**, *126*, 46–57. [CrossRef]
10. Toth, A.; Zhao, J. Evaluation of EPB TBM performance in mixed ground conditions. In Proceedings of theWorld Tunnel Congress (WTC)/General Assembly of the International-Tunnelling-and-Underground-Space-Association (ITA) 2013: Underground-The Way to the Future, Geneva, Switzerland, 31 May–7 June 2013; CRC Press: Boca Raton, FL, USA, 2013; pp. 1149–1156.
11. Zhou, X.P.; Zhai, S.F. Estimation of the cutterhead torque for earth pressure balance TBM under mixed-face conditions. *Tunn. Undergr. Space Technol.* **2018**, *74*, 217–229. [CrossRef]
12. Zhao, Y.; Gong, Q.; Tian, Z.; Zhou, S.; Jiang, H. Torque fluctuation analysis and penetration prediction of EPB TBM in rock–soil interface mixed ground. *Tunn. Undergr. Space Technol.* **2019**, *91*, 103002. [CrossRef]
13. Zhang, K.; Yu, H.; Liu, Z.; Lai, X. Dynamic characteristic analysis of TBM tunnelling in mixed-face conditions. *Simul. Model. Pract. Theory* **2010**, *18*, 1019–1031. [CrossRef]
14. Shi, H.; Yang, H.; Gong, G.; Wang, L. Determination of the cutterhead torque for EPB shield tunneling machine. *Autom. Constr.* **2011**, *20*, 1087–1095. [CrossRef]
15. Godinez, R.; Yu, H.; Mooney, M.; Gharahbagh, E.A.; Frank, G. Earth pressure balance machine cutterhead torque modeling: Learning from machine data. In Proceedings of the 2015 Rapid Excavation and Tunneling Conference, New Orleans, LA, USA, 7–10 June 2015; pp. 1261–1271.
16. Koohsari, A.; Kalatehjari, R.; Moosazadeh, S.; Hajihassani, M.; Tarafrava, M. Measurement and enhancing prediction of EPBM torque using actual Machine data. *Measurement* **2023**, *223*, 113780. [CrossRef]
17. Xu, Q.; Zhu, H.; Ding, W.; Wu, X.; Yu, N. Cutting torque during tunnelling process of earth pressure balance shield machine in homogeneous ground. *Chin. J. Geotech. Eng.* **2010**, *32*, 47–54. (In Chinese)
18. Lin, J. Study on Reduction of Cutterhead Torque in EPB Shield with Soil Conditioning. Ph.D. Thesis, Hohai University, Nanjing, China, 2006.

19. Zhang, Q.; Hou, Z.; Huang, G.; Cai, Z.; Kang, Y. Mechanical characterization of the load distribution on the cutterhead–ground interface of shield tunneling machines. *Tunn. Undergr. Space Technol.* **2015**, *47*, 106–113. [CrossRef]
20. Krause, T. *Schildvortrieb mit Flüssigkeits- und Erdgestützter Ortsbrust*; Mitteilungen des Instituts für Grundbau und Bodenmechanik der Technischen Universität Braunschweig; Technischen Universität Braunschweig: Braunschweig, Germany, 1987. (In German)
21. Avunduk, E.; Copur, H. Empirical modeling for predicting excavation performance of EPB TBM based on soil properties. *Tunn. Undergr. Space Technol.* **2018**, *71*, 340–353. [CrossRef]
22. Ramoni, M.; Anagnostou, G. The interaction between shield, ground and tunnel support in TBM tunnelling through squeezing ground. *Rock Mech. Rock Eng.* **2011**, *44*, 37–61. [CrossRef]
23. Ramoni, M.; Anagnostou, G. Tunnel boring machines under squeezing conditions. *Tunn. Undergr. Space Technol.* **2010**, *25*, 139–157. [CrossRef]
24. Zhang, Q.; Qu, C.; Cai, Z.; Kang, Y.; Huang, T. Modeling of the thrust and torque acting on shield machines during tunneling. *Autom. Constr.* **2014**, *40*, 60–67. [CrossRef]
25. Sterling, R.L. Developments and research directions in pipe jacking and microtunneling. *Undergr. Space* **2020**, *5*, 1–19. [CrossRef]
26. Deng, Z.; Liang, N.; Liu, X.; de la Fuente, A.; Lin, P.; Peng, H. Analysis and application of friction calculation model for long-distance rock pipe jacking engineering. *Tunn. Undergr. Space Technol.* **2021**, *115*, 104063. [CrossRef]
27. Deng, Z.; Liu, X.; Zhou, X.; Yang, Q.; Chen, P.; de la Fuente, A.; Ren, L.; Du, L.; Han, Y.; Xiong, F.; et al. Main engineering problems and countermeasures in ultra-long-distance rock pipe jacking project: Water pipeline case study in Chongqing. *Tunn. Undergr. Space Technol.* **2022**, *123*, 104420. [CrossRef]
28. Guo, R.; Jiang, H. Force and deformation of a shallow soil-buried super-long box culvert during jacking construction on a highway. *J. Highw. Transp. Res. Dev.* **2018**, *12*, 38–42. [CrossRef]
29. Zhang, P.; Ma, B.; Zeng, C.; Xie, H.; Li, X.; Wang, D. Key techniques for the largest curved pipe jacking roof to date: A case study of Gongbei tunnel. *Tunn. Undergr. Space Technol.* **2016**, *59*, 134–145. [CrossRef]
30. Hollmann, F.S.; Thewes, M. Assessment method for clay clogging and disintegration of fines in mechanised tunnelling. *Tunn. Undergr. Space Technol.* **2013**, *37*, 96–106. [CrossRef]

Disclaimer/Publisher's Note: The statements, opinions and data contained in all publications are solely those of the individual author(s) and contributor(s) and not of MDPI and/or the editor(s). MDPI and/or the editor(s) disclaim responsibility for any injury to people or property resulting from any ideas, methods, instructions or products referred to in the content.